Holo-lipocalin-2–derived siderophores increase mitochondrial ROS and impair oxidative phosphorylation in rat cardiomyocytes

Erfei Song[a], Sofhia V. Ramos[b], Xiaojing Huang[c], Ying Liu[d], Amy Botta[a], Hye Kyoung Sung[a], Patrick C. Turnbull[b], Michael B. Wheeler[d,e], Thorsten Berger[f,g], Derek J. Wilson[c], Christopher G. R. Perry[b], Tak W. Mak[f,g,1], and Gary Sweeney[a,1]

[a]Department of Biology, York University, Toronto, ON M3J 1P3, Canada; [b]Muscle Health Research Centre, School of Kinesiology and Health Science, York University, Toronto, ON M3J 1P3, Canada; [c]Department of Chemistry, York University, Toronto, ON M3J 1P3, Canada; [d]Department of Advanced Diagnostics, Toronto General Hospital Research Institute, University Health Network, Toronto, ON M5G 2M9, Canada; [e]Department of Physiology, University of Toronto, Toronto, ON M5S 1A8, Canada; [f]The Campbell Family Institute for Breast Cancer Research, University Health Network, Toronto, ON M5G 2M9, Canada; and [g]Ontario Cancer Institute, University Health Network, Toronto, ON M5G 2M9, Canada

Contributed by Tak W. Mak, December 29, 2017 (sent for review November 27, 2017; reviewed by Yan Chen and Kostas Pantopoulos)

Lipocalin-2 (Lcn2), a critical component of the innate immune response which binds siderophores and limits bacterial iron acquisition, can elicit spillover adverse proinflammatory effects. Here we show that holo-Lcn2 (Lcn2–siderophore–iron, 1:3:1) increases mitochondrial reactive oxygen species (ROS) generation and attenuates mitochondrial oxidative phosphorylation in adult rat primary cardiomyocytes in a manner blocked by *N*-acetyl-cysteine or the mitochondria-specific antioxidant SkQ1. We further demonstrate using siderophores 2,3-DHBA (2,3-dihydroxybenzoic acid) and 2,5-DHBA that increased ROS and reduction in oxidative phosphorylation are direct effects of the siderophore component of holo-Lcn2 and not due to apo-Lcn2 alone. Extracellular apo-Lcn2 enhanced the potency of 2,3-DHBA and 2,5-DHBA to increase ROS production and decrease mitochondrial respiratory capacity, whereas intracellular apo-Lcn2 attenuated these effects. These actions of holo-Lcn2 required an intact plasma membrane and were decreased by inhibition of endocytosis. The hearts, but not serum, of Lcn2 knockout (LKO) mice contained lower levels of 2,5-DHBA compared with wild-type hearts. Furthermore, LKO mice were protected from ischemia/reperfusion-induced cardiac mitochondrial dysfunction. Our study identifies the siderophore moiety of holo-Lcn2 as a regulator of cardiomyocyte mitochondrial bioenergetics.

lipocalin-2 | siderophore | iron | reactive oxygen species | NGAL

Defective myocardial energy metabolism is a major cause of heart failure and, as such, represents a long-standing therapeutic target (1, 2). In particular, a shift toward glycolysis, rather than mitochondrial oxidative metabolism, is important in the development of cardiac energy insufficiency leading to heart failure (3). An increase in reactive oxygen species (ROS) emanating from sources such as mitochondria, xanthine oxidase, or nicotinamide adenine dinucleotide phosphate oxidase (NADPH) has been proposed as a central driver of myocardial metabolic defects (4). Thus, enhancing our knowledge of the mechanisms leading to mitochondrial dysfunction could lead to new therapeutic strategies.

Recent work has increased our appreciation of the importance of bacteria–host interactions in controlling metabolism (5). Bacteria rely on secretion of siderophores to obtain iron from the infected host (6, 7). A host innate immune response involves neutrophil secretion of the siderophore-sequestering protein lipocalin-2 (previously known as siderocalin) (8). Elevated circulating Lcn2 levels strongly correlate with various forms of heart failure (9), and Lcn2 knockout (LKO) mice are protected from developing cardiovascular diseases by mechanisms that are not yet fully understood (10). Although our knowledge of how the gut microbiome influences human physiology has grown exponentially (11), it has been speculated that specific tissue microbiomes exist that may influence susceptibility to disease development (12).

Gut microbiota composition can influence development of heart disease, but a more mechanistic understanding of this correlation is needed (13, 14). One example of bacteria–host communication involves the release of trimethylamine-*N*-oxide and short-chain fatty acids (13, 15). Another possibility may be siderophores, which can have direct cellular effects such as stabilizing the hypoxia-inducible factor (HIF) transcription factors responsible for secretion of proinflammatory cytokines (16–18). Increasing our understanding of crosstalk between bacteria and the host, and the role of innate immunity, could provide valuable insights for guiding current interest in prebiotics (19) and postbiotics (20) as agents to treat metabolic disease.

In this study, we compared the effects of apo-Lcn2 and holo-Lcn2 on mitochondrial respiration and ROS generation in adult rat primary cardiomyocytes, examined siderophore contents of the circulation and heart tissues of WT and LKO mice, and tested mitochondrial respiration in WT and mutant hearts subjected to ischemia/reperfusion (IR) injury. Our data provide new

Significance

Metabolic dysfunction associated with decreased mitochondrial oxidative capacity is a major underlying cause of heart failure. Our study sheds new light on the potential role of bacteria-derived or endogenous siderophores as direct regulators of cardiomyocyte mitochondrial function. Furthermore, we demonstrate that lipocalin-2, a key feature of the innate immune response, facilitates the transport of siderophore–iron complexes into cells. This mechanism may have important physiological implications because elevated lipocalin-2 levels correlate positively with heart failure in humans, and mice lacking lipocalin-2 are protected from stress-induced mitochondrial dysfunction and heart failure.

Author contributions: E.S., S.V.R., X.H., Y.L., A.B., H.K.S., P.C.T., M.B.W., D.J.W., C.G.R.P., T.W.M., and G.S. designed research; E.S., S.V.R., X.H., Y.L., A.B., H.K.S., P.C.T., M.B.W., D.J.W., and C.G.R.P. performed research; E.S., T.B., and T.W.M. contributed new reagents/analytic tools; E.S., S.V.R., X.H., Y.L., A.B., H.K.S., P.C.T., M.B.W., D.J.W., C.G.R.P., T.W.M., and G.S. analyzed data; and E.S., S.V.R., X.H., A.B., H.K.S., P.C.T., M.B.W., T.B., D.J.W., C.G.R.P., and G.S. wrote the paper.

Reviewers: Y.C., Chinese Academy of Sciences; and K.P., Lady Davis Institute for Medical Research, McGill University.

The authors declare no conflict of interest.

[1]To whom correspondence may be addressed. Email: tmak@uhnres.utoronto.ca or gsweeney@yorku.ca.

This article contains supporting information online at www.pnas.org/lookup/suppl/doi:10.1073/pnas.1720570115/-/DCSupplemental.

insight into holo-Lcn2 actions and identify the potential importance of siderophores in cardiac disease development.

Results

Apo-Lcn2 and Holo-Lcn2 Have Differing Effects on Mitochondrial Respiration and ROS Generation in Rat Cardiomyocytes. *Escherichia coli* strains BL21 and XL1-Blue were used to produce recombinant apo-Lcn2 (without siderophores or iron) (Fig. 1*A*) and holo-Lcn2 (with siderophores and iron) (Fig. 1*B*), respectively (21, 22). The native mass spectrum of holo-Lcn2 purified from XL1-Blue indicated a specific holo-protein complex corresponding to apo-Lcn2 protein bound to three 2,3-DHBA (2,3-dihydroxybenzoic acid) molecules and one iron molecule (Fig. 1*B*). Although no structure is available for mouse holo-Lcn2, its arrangement is expected to be homologous to the human protein–2,3-DHBA–iron complex. Next, we used high-resolution respirometry (Oxygraph-2k; O2k; Oroboros Instruments) to examine the effects on mitochondrial respiration of treating cultured rat primary adult cardiomyocytes with 1 μg/mL recombinant apo- or holo-Lcn2. As indicated in the respiratory traces shown in Fig. 1 *C* and *D*, treatment with holo-Lcn2 significantly decreased ADP-stimulated mitochondrial respiration when supported by complex I (NADH from pyruvate/malate and glutamate) and complex II ($FADH_2$, succinate). In contrast, treatment with apo-Lcn2 did not exert any deleterious effect on mitochondrial respiration. Western blot analysis revealed increased protein expression of complex II in the multiprotein OXPHOS complex (Fig. 1 *E* and *F*), suggesting that a compensatory mechanism is activated upon respiratory suppression by holo-Lcn2.

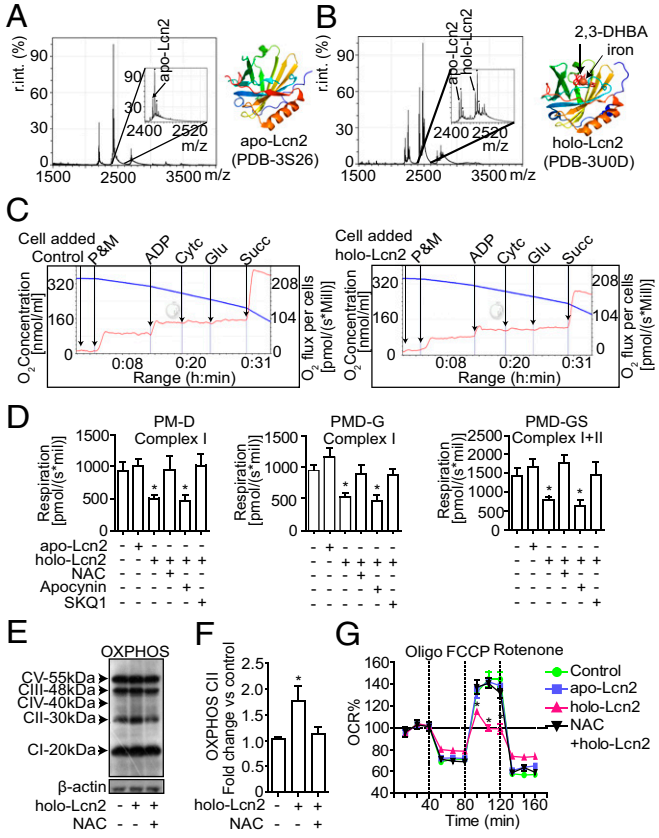

Fig. 1. Holo-Lcn2 decreases mitochondrial respiration in rat primary cardiomyocytes. (*A* and *B*) MS analysis of recombinant apo-Lcn2 (*A*) and holo-Lcn2 (*B*) proteins. Compared with apo-Lcn2, the mass of holo-Lcn2 was increased by 517 Da and corresponded approximately to three DHBA molecules (3 × 154 Da) and one iron molecule (56 Da). Protein Data Bank (PDB) simulation of holo-Lcn2 shows Lcn2 protein present with DHBA and iron in a 1:3:1 ratio. r.int. (%), percentage of relative intensity. (*C*) Representative O2k traces detecting O_2 consumption in rat primary cardiomyocytes treated without (*Left*) or with holo-Lcn2 (*Right*) for 2 h. Cytc, cytochrome c. (*D*) Quantitation by O2k assay of cardiomyocyte respiration that was stimulated by ADP (D; 5 mM) and supported by pyruvate (P; 5 mM; *Left*), glutamate (G; 5 mM; *Center*), or succinate (S; 20 mM; *Right*) in the presence of malate (M; 0.5 mM). Respiration was evaluated after 2-h treatment (+) or not (–) with 1 μg/mL apo-Lcn2 or holo-Lcn2 in the presence (+) (30-min pretreatment) or absence (–) of the ROS inhibitors NAC (500 nM), apocynin (100 μM), or SkQ1 (20 nM), as indicated (n = 8). (*E* and *F*) Western blot analysis (*E*) and quantitation (*F*) of changes to mitochondrial OXPHOS complexes in cardiomyocytes treated with holo-Lcn2 in the presence or absence of NAC, as indicated (n = 4). β-Actin, loading control. (*G*) Oxygen consumption rate (OCR) as measured by Seahorse XF^{e}24 Analyzer of H9C2 cells treated for 2 h with 1 μg/mL apo-Lcn2 or holo-Lcn2 in the absence or presence (30-min pretreatment) of NAC (500 nM), as indicated (n = 3). Quantitative data are the mean ± SEM and *P < 0.05 versus control.

Lcn2 has been shown to increase ROS production (23). Accordingly, we found that pretreatment of cardiomyocytes with *N*-acetyl-cysteine (NAC), a general ROS inhibitor, attenuated the decrease in mitochondrial respiration induced by holo-Lcn2 (Fig. 1*D*). To further investigate the source of ROS associated with holo-Lcn2 function, we pretreated cardiomyocytes with apocynin, a specific NADPH oxidase inhibitor, or SkQ1, a specific inhibitor of mitochondrial ROS production (24). SkQ1, but not apocynin, prevented the reduction in mitochondrial function induced by holo-Lcn2 (Fig. 1*D*). To validate the differential effects of apo- versus holo-Lcn2 on mitochondrial respiration, we used the Seahorse XF method to measure changes to respiration in the embryonic ventricular cardiomyocyte cell line H9C2. We obtained similar results in that only holo-Lcn2 treatment significantly reduced mitochondrial respiration in H9C2 cells (Fig. 1*G*).

To visualize ROS production, we used the CellROX Green probe (25), which detects both superoxide and H_2O_2 and is engineered to bind to DNA, and thus fluorescence appears mainly nuclear or mitochondrial. We found that treatment with holo-Lcn2, but not apo-Lcn2, induced ROS generation in cultured cardiomyocytes (Fig. 2 *A* and *B*). Both immunofluorescent images and quantitative analysis showed this was attenuated by addition of NAC or SkQ1 but not apocynin. Similar results were observed when the ROS fluorophore DCF-DA (2,7-dichlorodihydrofluorescein diacetate) (26) was used to determine ROS production in H9C2 cells (Fig. 2*C*).

Siderophore Functions Underlie the Differential Effects of Apo- and Holo-Lcn2 on Mitochondrial Respiration. The holo-Lcn2 used in our cardiomyocyte experiments contained apo-Lcn2 protein plus 2,3-DHBA (siderophore) and iron, which led us to propose that the distinct effects on cells of holo-Lcn2 must be due to the presence of either the iron or siderophore. High concentrations of iron can induce ROS production (27), making it logical to hypothesize that iron present in holo-Lcn2 might trigger ROS generation leading to mitochondrial dysfunction. We found that ferric iron, used at an amount equimolar to that in 1 μg/mL holo-Lcn2 (50 nM), did not reduce mitochondrial respiration as measured by O2k analysis (Fig. 3*A*). It is likely that the free iron-binding capacity of ferritin in the cytosol easily buffered this amount of iron. When we pretreated cardiomyocytes with the iron chelator 2,2′-bipyridyl (DPD), the effects of holo-Lcn2 treatment were not prevented, further suggesting that iron does not play a role (Fig. 3*A*). Moreover, ferric iron treatment did not result in significant ROS production, and DPD pretreatment did not inhibit holo-Lcn2–induced ROS generation (Fig. 3*B*). A potential limitation of this work is lacking combined use of powerful chelators of Fe^{2+} and Fe^{3+}. Treatment of primary cardiomyocytes with holo-Lcn2 or 50 nM ferric iron did not significantly alter the level of intracellular ferritin whereas, as expected, positive control of higher-dose $FeSO_4$ did (Fig. 3*C*).

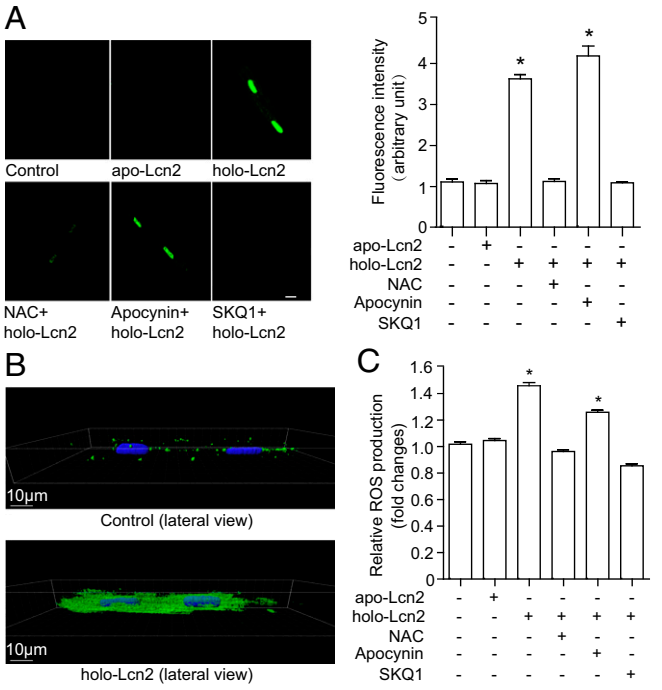

Fig. 2. Elevated ROS production induced by holo-Lcn2 is attenuated by a mitochondrial ROS inhibitor. (*A*) Rat primary cardiomyocytes were preincubated for 30 min with the indicated ROS inhibitors before 2-h treatment with apo- or holo-Lcn2. (*A*, *Left*) Representative fluorescent imaging of oxidative stress in these cells as detected by the CellROX Green assay. (*A*, *Right*) Quantitation of fluorescence intensities in the images (*Left*) by ImageJ (NIH) ($n = 3$). (Scale bar: 20 μm.) (*B*) Representative 3D confocal images of the cardiomyocytes in *A* that were treated with holo-Lcn2 and stained with CellROX Green. (*C*) Quantitation of DCF-DA analysis of ROS production by H9C2 cells treated with apo- or holo-Lcn2 in the presence/absence of the indicated inhibitors as in *A* ($n = 4$). Quantitative data are the mean ± SEM and $^*P < 0.05$ versus control.

We next tested the ability of siderophores to inhibit mitochondrial respiration in primary cardiomyocytes. 2,3-DHBA is produced by many bacteria, while 2,5-DHBA has been proposed to be an endogenous mammalian siderophore (21, 28). Data obtained from both O2k and Seahorse analyses showed a decrease in cardiomyocyte mitochondrial respiratory capacities in response to 50 nM 2,3-DHBA [pyruvate malate and ADP (PM-D), $P = 0.076$; pyruvate malate ADP and glutamate (PMD-G), $P = 0.067$; and significant for pyruvate malate ADP glutamate and succinate (PMD-GS)] or 2,5-DHBA (significant for PM-D, PMD-G, and PMD-GS) treatment (Fig. 3 *D* and *E*). Of note, the magnitude observed was less than in cells treated with holo-Lcn2. In contrast to 2,3-DHBA or 2,5-DHBA, exposure to 50 nM pyoverdine, a siderophore that does not bind to Lcn2, did not significantly elevate intracellular ROS (Fig. 3 *F* and *K*). Treatment of permeabilized cardiomyocytes with 50 nM 2,3-DHBA markedly decreased respiration (O2k) in the absence of ADP, suggesting that 2,3-DHBA acutely induced a proton leak possibly through an uncoupling mechanism (Fig. 3*G*). Pretreatment of cells with apo-Lcn2 to allow its internalization and an increase in its intracellular level prevented ROS production in response to 2,3-DHBA, whereas cotreatment of cells with 2,3-DHBA plus apo-Lcn2 (such that apo-Lcn2 and 2,3-DHBA bound together extracellularly and were internalized via receptor-mediated endocytosis) enhanced ROS production (Fig. 3*H*). In keeping with this observation, apo-Lcn2 potentiated the effects of 2,3-DHBA, 2,5-DHBA, and enterobactin on ROS generation at concentrations less than 50 nM (Fig. 3 *I*–*K*). These data imply that Lcn2 has an important facilitatory role in DHBA-induced ROS production and impairment of mitochondrial respiration.

The Effects of Holo-Lcn2 on Mitochondria Depend on Receptor-Mediated Endocytosis. Two putative receptors of Lcn2 are 24p3R and megalin (29). When we treated permeabilized cardiomyocytes with holo-Lcn2, no changes to mitochondrial respiration were observed (Fig. 4*A*). These data suggested that an intact cell membrane and binding between Lcn2 and a receptor

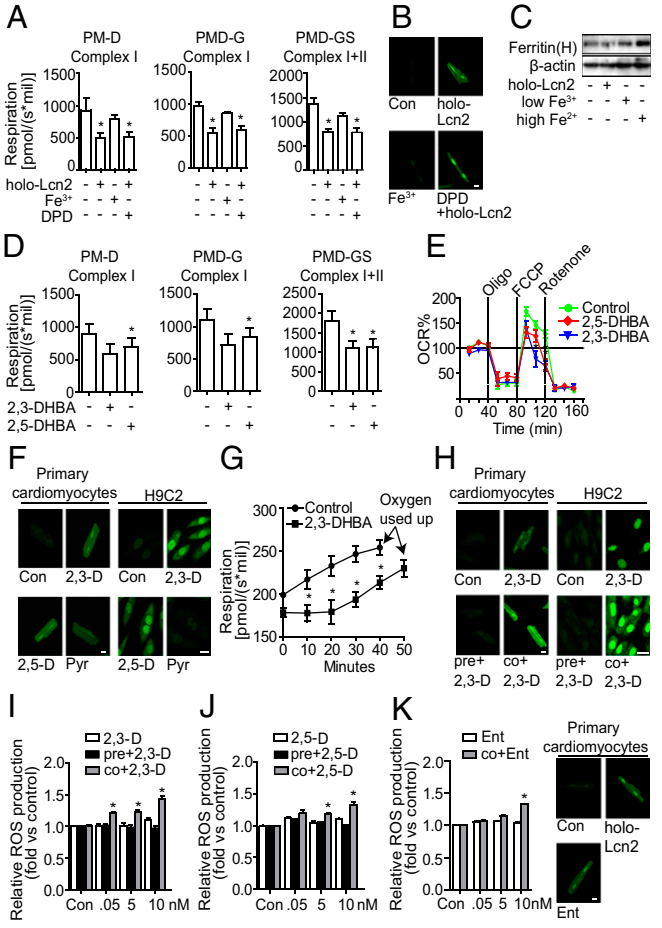

Fig. 3. Apo-Lcn2 potentiates DHBAs to decrease mitochondrial respiration and enhance ROS production. (*A*) Quantitation of O2k analysis conducted as in Fig. 1*D* of respiration in primary cardiomyocytes treated with holo-Lcn2 (1 μg/mL), Fe^{3+} (50 nM), and/or DPD (100 μM), as indicated ($n = 4$). (*B*) Representative CellROX Green analysis of ROS production by primary cardiomyocytes. (Scale bar: 20 μm.) (*C*) Western blot to detect ferritin in primary cardiomyocytes treated with holo-Lcn2 (1 μg/mL), Fe^{3+} (50 nM), or Fe^{2+} (100 μM; positive control), as indicated. (*D*) Quantitation of O2k analysis in primary cardiomyocytes treated with 50 nM 2,3-DHBA or 2,5-DHBA ($n = 5$). (*E*) Quantitation of OCR traces measured by Seahorse assay using H9C2 cells treated with 50 nM 2,3-DHBA or 2,5-DHBA ($n = 3$). FCCP, carbonyl cyanide-*p*-trifluoromethoxyphenylhydrazone. (*F*) Representative CellROX Green analysis of ROS production by primary cardiomyocytes and H9C2 cells treated with 50 nM 2,3-DHBA (2,3-D), 2,5-DHBA (2,5-D), or pyoverdine (Pyr). (Scale bar: 20 μm.) (*G*) Quantitation of O2k analysis conducted as in *A* of proton leak in primary cardiomyocytes treated with 2,3-DHBA (50 nM) ($n = 7$). (*H*) Representative CellROX Green analysis of ROS production by primary cardiomyocytes or H9C2 cells that were pretreated (pre) with apo-Lcn2 before treatment with 2,3-DHBA (50 nM) or cotreated (co) with apo-Lcn2 plus 2,3-DHBA (50 nM). (Scale bar: 20 μm.) (*I* and *J*) Quantitation of 2,7-dichlorodihydrofluorescein diacetate (DC-FDA) analysis of ROS production by H9C2 cells either pretreated or cotreated with apo-Lcn2 as in *H* in conjunction with the indicated concentrations of 2,3-DHBA (*I*) or 2,5-DHBA (*J*) ($n = 4$). (*K*, *Left*) Quantitation of DC-FDA analysis of ROS production by H9C2 cells cotreated with apo-Lcn2 plus enterobactin (50 nM; Ent.), as indicated ($n = 4$). (*K*, *Right*) Representative CellROX Green analysis of ROS production. (Scale bar: 20 μm.) Quantitative data are the mean ± SEM and $^*P < 0.05$ versus control.

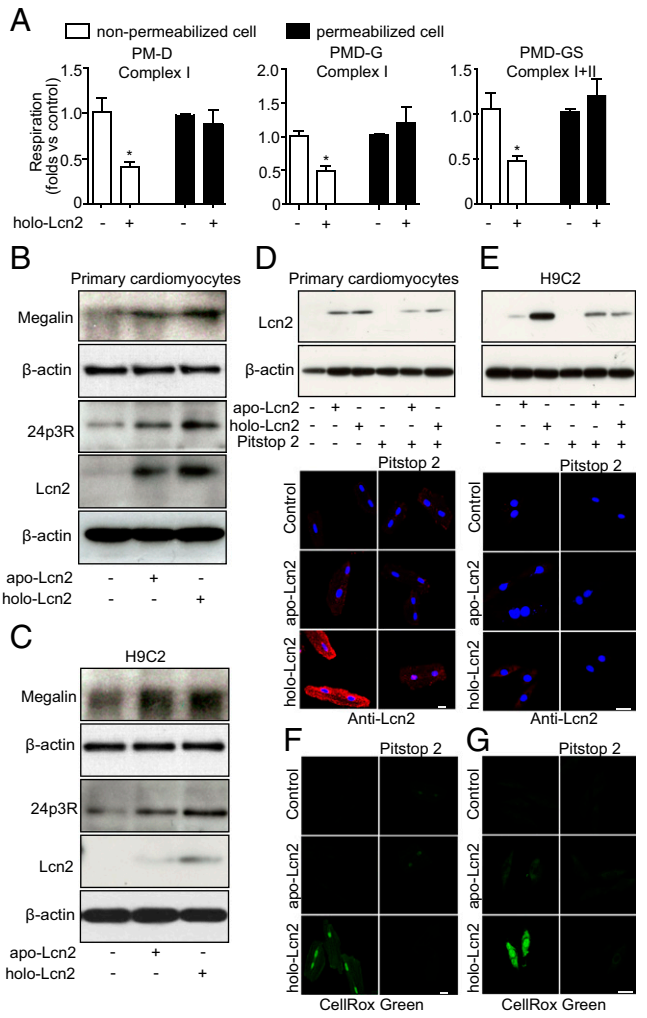

Fig. 4. Inhibition of endocytosis attenuates the decrease in mitochondrial respiration induced by holo-Lcn2. (*A*) O2k analysis as in Fig. 1*D* of mitochondrial respiration in primary cardiomyocytes that underwent permeabilization (or not) and were treated with holo-Lcn2 ($n = 3$). (*B* and *C*) Western blot to detect the indicated proteins in primary cardiomyocytes (*B*) and H9C2 cells (*C*) treated with 1 μg/mL apo- or holo-Lcn2, as indicated. (*D* and *E*) Western blot (*Top*) and immunofluorescence staining (*Bottom*) analyses to detect Lcn2 in primary cardiomyocytes (*D*) and H9C2 cells (*E*) pretreated with Pitstop 2 (10 μM) and treated with apo- or holo-Lcn2, as indicated. (*F* and *G*) Representative CellROX Green analyses of ROS production by the cells in *D* and *E*, respectively. Quantitative data are the mean ± SEM and $^*P < 0.05$ versus control. (Scale bars: *D*–*G*, 20 μm.)

are needed for holo-Lcn2's effects. Western blot analysis revealed that treatment with holo-Lcn2 (but not apo-Lcn2) increased megalin and 24p3R protein levels in both primary cardiomyocytes and H9C2 cells (Fig. 4 *B* and *C*). We then pretreated cells with Pitstop 2, an inhibitor of clathrin-mediated endocytosis, and found that the internalization of apo- and holo-Lcn2 were significantly reduced in both cell types (Fig. 4 *D* and *E*). Importantly, holo-Lcn2–induced ROS production was also markedly attenuated by Pitstop 2 pretreatment (Fig. 4 *F* and *G*).

At the molecular level, determination of native electrospray mass spectra at pH 2.5 indicated that the apo-Lcn2 and holo-Lcn2 proteins remain folded even under low-pH conditions (Fig. 5 *A* and *B*). We incubated purified apo-Lcn2 protein with various siderophores and used mass spectrometry (MS) to determine in vitro binding affinities. We found that apo-Lcn2 was able to bind to 2,3-DHBA and enterobactin in vitro (Fig. 5 *C* and *D*). Somewhat surprisingly, it did not bind to 2,5-DHBA or pyoverdine, likely due to the in vitro conditions used (Fig. 5 *E* and *F*).

Hearts of LKO Mice Show Reduced Siderophore Content and IR-Induced Mitochondrial Respiratory Dysfunction. Previous studies have established that cardiac function in LKO mice is enhanced compared with that in WT controls (30). Using O2k analysis, we determined that hearts of LKO mice tended to exhibit increased mitochondrial respiration, but this difference from WT controls was not statistically significant (Fig. 6*A*). After IR challenge via coronary artery ligation, mitochondrial respiration capacities in terms of ADP- (total), glutamate- (complex I), and succinate- (complex II) driven respiration were largely preserved in LKO mice (Fig. 6*A*). Based on the striking impact on mitochondrial function of 2,3-DHBA and 2,5-DHBA, we then examined heart tissues and sera of untreated WT and LKO mice using MS. LKO hearts showed a lower total DHBA content than WT hearts, but the relative levels of these siderophores in sera of WT and mutant mice were comparable (Fig. 6 *B*–*D*). These results suggest the intriguing possibility that it is the delivery of siderophores into heart tissue by holo-Lcn2 that disrupts cardiomyocyte metabolism and sets the stage for heart failure.

Discussion

Metabolic dysfunction is a prominent pathophysiological feature of heart failure, and LKO mice are protected from heart failure induced by various stresses (10, 30). An increase in circulating Lcn2 is observed in obese patients with metabolic disorders as well as in patients with various forms of heart failure (31, 32). Previous studies using mouse models of heart failure have revealed decreased mitochondrial damage in LKO hearts compared with WT

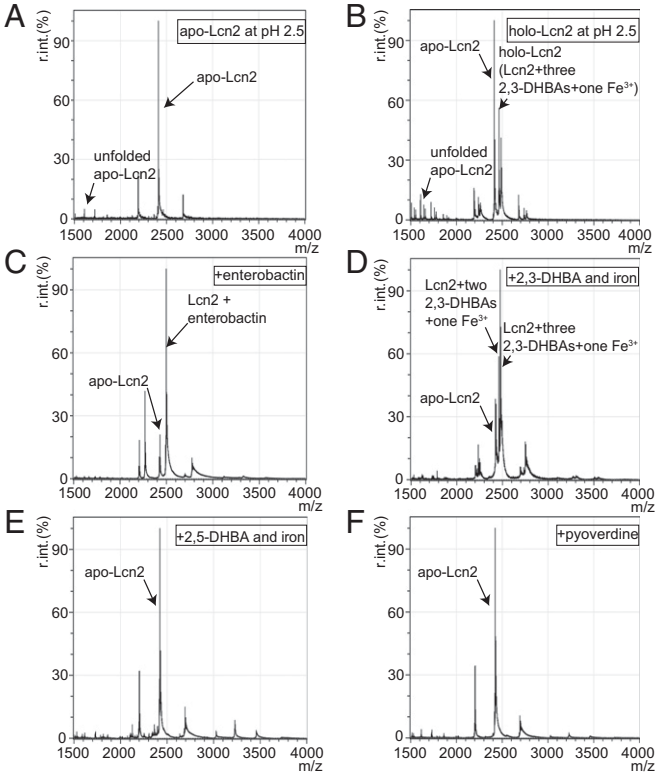

Fig. 5. In vitro binding affinities of apo-Lcn2 for siderophores. (*A* and *B*) MS analyses of recombinant (*A*) apo-Lcn2 and (*B*) holo-Lcn2 at pH 2.5. (*C*–*F*) MS analyses of binding in vitro between apo-Lcn2 and (*C*) enterobactin, (*D*) 2,3-DHBA plus iron, (*E*) 2,5-DHBA plus iron, and (*F*) pyoverdine at the ratios described in *SI Methods*.

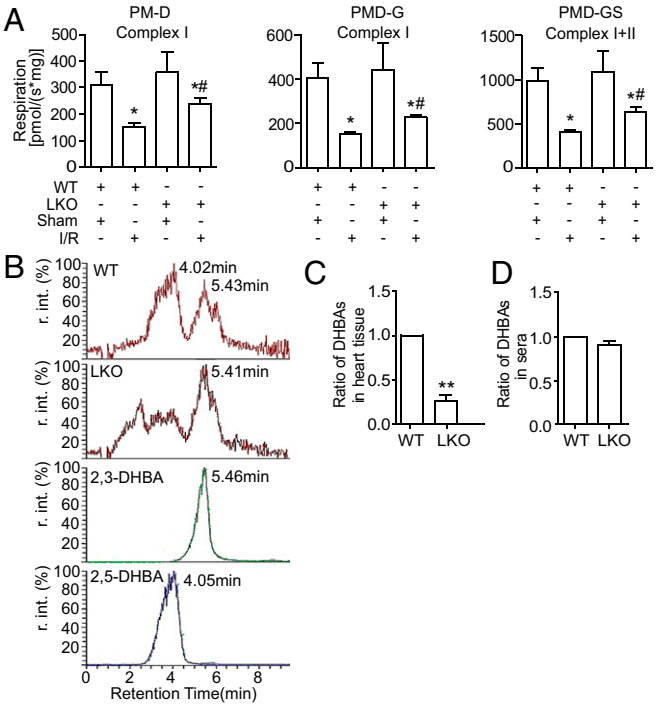

Fig. 6. Hearts of LKO mice have a lower DHBA content and less mitochondrial damage after IR injury. (*A*) Quantitation of O2k analysis as in Fig. 1*D* of respiration in heart tissue fibers prepared from WT and LKO mice, with (I/R) or without (sham) IR challenge. $^{*}P < 0.05$ versus sham group; $^{\#}P < 0.05$ versus WT-IR ($n = 6$). (*B*, *Top* two panels) Representative MS traces measuring relative DHBA content in whole hearts of WT and LKO mice ($n = 3$). (*B*, *Bottom* two panels) MS traces of solutions of 2,3-DHBA (10 μM) and 2,5-DHBA (10 μM) used as standards for validation of retention time and *m/z* (153.0193 negative ionization mode). (*C* and *D*) Relative ratio of total DHBAs in hearts (*C*) and sera (*D*) of WT and LKO mice. $^{**}P < 0.01$ versus sham group ($n = 3$). Quantitative data are the mean ± SEM.

controls (30). Our findings show that the holo-Lcn2 complex containing siderophores and iron enters cardiomyocytes and can directly modulate mitochondrial bioenergetics. Treatment with exogenous holo-Lcn2 inhibits complex I- and II-mediated respiration in cultured adult rat primary cardiomyocytes. The prevention of this impairment by the mitochondria-targeted antioxidant SkQ1 demonstrates that siderophores induce the generation of substantial mitochondrial ROS that impair oxidative energy production. Furthermore, this inhibitory effect is directly due to the siderophore component of holo-Lcn2, as neither the Lcn2 moiety (apo-Lcn2) nor the low concentrations of iron in this complex on its own altered mitochondrial bioenergetics. Higher levels of iron, such as in iron overload conditions, can of course impact mitochondrial function. Moreover, treatment of cells with purified siderophores mimicked the effects of holo-Lcn2. These data are in line with the observation that LKO mice show a reduced degree of inhibition of mitochondrial respiration following IR injury. Given the known link between mitochondrial dysfunction and cardiomyopathy induced by IR (33), our work now suggests that siderophore production by the host or microbiome may contribute to cardiac dysfunction by impairing cardiac mitochondrial bioenergetics.

ROS production is rapidly elevated upon infection as part of the innate immune response (34). In addition to harming microbes that invade tissues, these increased ROS act as secondary messengers signaling for inflammatory and immune responses (35). Neutrophils can generate ROS after their surface *N*-formyl peptide receptors make contact with the *N*-formyl groups of bacterial proteins (36). In addition to producing ROS, a mammalian host fights infection by up-regulating Lcn2, the major function of which is to prevent invading bacteria from acquiring host iron. To thrive after infecting a host, bacteria secrete various siderophores that capture host iron (37). The apo-Lcn2 protein binds to these siderophores with their captured iron, creating the holo-Lcn2 complex that is associated with bacterial demise. However, our work has shown that the siderophore component of holo-Lcn2 can contribute to mitochondrial dysfunction in cardiomyocytes. Indeed, in our experiments, the holo-Lcn2 complex itself was more potent in decreasing mitochondrial respiration and ROS production than was any siderophore alone. Our data obtained using the antioxidant SkQ1 demonstrate that siderophores accumulating in cardiac tissue can elicit ROS generation by mitochondria. In this light, it is interesting to note that, although mitochondria originated in bacteria (38), the specific sites targeted by siderophores to induce ROS generation remain unclear.

Concentrations of 2,5-DHBA are reduced in hearts of LKO mice, and 2,5-DHBA has been proposed as the only endogenous mammalian siderophore able to bind to Lcn2 (21, 28). Interestingly, although this interaction occurs in vivo, we found that purified recombinant Lcn2 did not bind to 2,5-DHBA in vitro. Understanding exactly how endogenous siderophores bind to Lcn2 is important because siderophores may have wide-ranging metabolic effects. The formation of endogenous 2,3- and 2,5-DHBAs is catalyzed in humans by the P450 enzymes, including the 2C8, 2C9, and 2C19 isoforms (39). Notably, when WT obese mice were treated with sulfaphenazole, a selective inhibitor of P450 2C9, endothelial function improved. This improvement was due to blockage of the effects of Lcn2 on aortic endothelial-dependent relaxation and contraction in response to insulin or acetylcholine, as well as endothelial NOS uncoupling, a process sensitive to ROS elevation (40). In this context, another interesting observation from our study is that pretreatment of cells with apo-Lcn2 to increase its intracellular level significantly reduces DHBA-induced ROS production, suggesting that intracellular apo-Lcn2 acts as a siderophore–iron chelator. When Lcn2 rises during infection or inflammation, the prevention of a response to DHBAs might be important to avoid further damage to the host. Indeed, LKO mice have a lower DHBA content and are protected from IR-induced mitochondrial dysfunction.

Levels of mitochondrial and cytosolic iron are tightly regulated by iron storage and transport proteins such as ferritin and mitoferrin-1 and -2 (41). High iron levels can elevate ROS, yet in our study treatment of cells with 50 nM $FeCl_3$ did not exert detrimental effects on respiration via ROS production, suggesting that the amount of iron delivered by 1 μg/mL holo-Lcn2 does not mediate effects of this complex. Unlike in bacteria, no cell-surface receptors for siderophores have been identified on mammalian cells, making it likely that Lcn2 is an important vehicle for bringing siderophores into cells. The unsuccessful treatment of pathogen-induced infections with siderophore-conjugate drugs implies that the amount of siderophore gaining entrance to a cell is critical to its effects (42). Furthermore, certain direct biological consequences of siderophore import are now beginning to be realized. Enterobactin stabilizes HIF-1α in respiratory cells in vitro, thereby inducing the expression of proinflammatory cytokines and enhancing Lcn2-mediated inflammation (18).

In summary, we have shown that holo-Lcn2, but not apo-Lcn2, induces mitochondrial ROS generation and suppresses oxidative phosphorylation in a manner mimicked by DHBAs but not by iron. This effect of holo-Lcn2 is not attenuated by iron chelation, indicating that siderophores can have direct effects on mitochondria. This identification of the interplay between Lcn2, iron, and siderophores in regulating cardiomyocyte mitochondrial bioenergetics may have important physiological implications, such that therapeutic targeting of this interplay may in the future decrease heart failure in susceptible patients.

Methods

Full details on the majority of methods are available in *Supporting Information*, with brief details given here.

Adult Wistar male rats (age 6 to 10 wk) were used for isolation of primary cardiomyocytes using a protocol approved by the Animal Care Committee at York University. Mitochondrial respiration was assessed in isolated cardiomyocytes using the high-resolution respirometer Oxygraph-2k (Oroboros Instruments) and in H9C2 cells with the XF^{e}24 Seahorse Metabolic Flux Analyzer (Agilent). ROS determination was performed using the CellROX or DCF-DA assay. Native mass spectra of apo- and holo-Lcn2 were captured on a Waters Synapt G2-S instrument. The LC-MS platform used to detect DHBAs consisted of a Dionex UltiMate 3000 UHPLC system and a Q Exactive mass spectrometer equipped with a HESI-II source (Thermo Scientific). Control of the system and data handling were performed using Thermo Xcalibur 2.2 software and Chromeleon 7.2 software. Liquid chromatography was conducted on a Hypersil Gold C18 column (Thermo Scientific). Ligation of the left anterior descending artery was used to induce ischemia/reperfusion injury in mice.

ACKNOWLEDGMENTS. This work was funded by grants from the Heart and Stroke Foundation of Canada (to G.S.); Natural Sciences and Engineering Research Council of Canada (436138-2013) (to C.G.R.P.); James H. Cummings Foundation (C.G.R.P.); Canadian Institutes of Health Research (CIHR; FDN-143219) (to M.B.W.); Canadian Foundation for Innovation and Ontario Research Fund (Project no. 30961); CIHR Postdoctoral Fellowship and York Science Postdoctoral Fellowship (to A.B.); and York Postdoctoral Fellowship (to H.K.S.). G.S. holds a Mid-Career Investigator Award from the Heart and Stroke Foundation.

1. Doenst T, Nguyen TD, Abel ED (2013) Cardiac metabolism in heart failure: Implications beyond ATP production. *Circ Res* 113:709–724.
2. Steggall A, Mordi IR, Lang CC (2017) Targeting metabolic modulation and mitochondrial dysfunction in the treatment of heart failure. *Diseases* 5:E14.
3. Lopaschuk GD (2017) Metabolic modulators in heart disease: Past, present, and future. *Can J Cardiol* 33:838–849.
4. Wilson AJ, et al. (September 27, 2017) Reactive oxygen species signalling in the diabetic heart: Emerging prospect for therapeutic targeting. *Heart*, 10.1136/heartjnl-2017-311448.
5. Sommer P, Sweeney G (2010) Functional and mechanistic integration of infection and the metabolic syndrome. *Korean Diabetes J* 34:71–76.
6. Cohen LJ, et al. (2017) Commensal bacteria make GPCR ligands that mimic human signalling molecules. *Nature* 549:48–53.
7. Cohen LJ, et al. (2015) Functional metagenomic discovery of bacterial effectors in the human microbiome and isolation of commendamide, a GPCR G2A/132 agonist. *Proc Natl Acad Sci USA* 112:E4825–E4834.
8. Moschen AR, Adolph TE, Gerner RR, Wieser V, Tilg H (2017) Lipocalin-2: A master mediator of intestinal and metabolic inflammation. *Trends Endocrinol Metab* 28:388–397.
9. Marques FZ, et al. (2017) Experimental and human evidence for lipocalin-2 (neutrophil gelatinase-associated lipocalin [NGAL]) in the development of cardiac hypertrophy and heart failure. *J Am Heart Assoc* 6:e005971.
10. Song E, et al. (2017) Lipocalin-2 induces NLRP3 inflammasome activation via HMGB1 induced TLR4 signaling in heart tissue of mice under pressure overload challenge. *Am J Transl Res* 9:2723–2735.
11. Koppel N, Balskus EP (2016) Exploring and understanding the biochemical diversity of the human microbiota. *Cell Chem Biol* 23:18–30.
12. Grasset E, et al. (2017) A specific gut microbiota dysbiosis of type 2 diabetic mice induces GLP-1 resistance through an enteric no-dependent and gut-brain axis mechanism. *Cell Metab* 25:1075–1090.e5, and erratum (2017) 26:278.
13. Zhu W, et al. (2016) Gut microbial metabolite TMAO enhances platelet hyperreactivity and thrombosis risk. *Cell* 165:111–124.
14. Tang WH, Hazen SL (2017) The gut microbiome and its role in cardiovascular diseases. *Circulation* 135:1008–1010.
15. Ahmadmehrabi S, Tang WHW (2017) Gut microbiome and its role in cardiovascular diseases. *Curr Opin Cardiol* 32:761–766.
16. Hartmann H, et al. (2008) Hypoxia-independent activation of HIF-1 by Enterobacteriaceae and their siderophores. *Gastroenterology* 134:756–767.
17. Palazon A, Goldrath AW, Nizet V, Johnson RS (2014) HIF transcription factors, inflammation, and immunity. *Immunity* 41:518–528.
18. Holden VI, et al. (2014) Bacterial siderophores that evade or overwhelm lipocalin 2 induce hypoxia inducible factor 1α and proinflammatory cytokine secretion in cultured respiratory epithelial cells. *Infect Immun* 82:3826–3836.
19. Hill C, et al. (2014) Expert consensus document. The International Scientific Association for Probiotics and Prebiotics consensus statement on the scope and appropriate use of the term probiotic. *Nat Rev Gastroenterol Hepatol* 11:506–514.
20. Ojeda P, Bobe A, Dolan K, Leone V, Martinez K (2016) Nutritional modulation of gut microbiota—The impact on metabolic disease pathophysiology. *J Nutr Biochem* 28:191–200.
21. Devireddy LR, Hart DO, Goetz DH, Green MR (2010) A mammalian siderophore synthesized by an enzyme with a bacterial homolog involved in enterobactin production. *Cell* 141:1006–1017.
22. Goetz DH, et al. (2002) The neutrophil lipocalin NGAL is a bacteriostatic agent that interferes with siderophore-mediated iron acquisition. *Mol Cell* 10:1033–1043.
23. Wu L, Du Y, Lok J, Lo EH, Xing C (2015) Lipocalin-2 enhances angiogenesis in rat brain endothelial cells via reactive oxygen species and iron-dependent mechanisms. *J Neurochem* 132:622–628.
24. Anisimov VN, et al. (2011) Effects of the mitochondria-targeted antioxidant SkQ1 on lifespan of rodents. *Aging (Albany NY)* 3:1110–1119.
25. Davison CA, et al. (2013) Antioxidant enzymes mediate survival of breast cancer cells deprived of extracellular matrix. *Cancer Res* 73:3704–3715.
26. Wu D, Yotnda P (2011) Production and detection of reactive oxygen species (ROS) in cancers. *J Vis Exp* (57):3357.
27. Dixon SJ, Stockwell BR (2014) The role of iron and reactive oxygen species in cell death. *Nat Chem Biol* 10:9–17.
28. Liu Z, et al. (2014) Regulation of mammalian siderophore 2,5-DHBA in the innate immune response to infection. *J Exp Med* 211:1197–1213.
29. Langelueddecke C, et al. (2012) Lipocalin-2 (24p3/neutrophil gelatinase-associated lipocalin (NGAL)) receptor is expressed in distal nephron and mediates protein endocytosis. *J Biol Chem* 287:159–169.
30. Yang B, et al. (2012) Improved functional recovery to I/R injury in hearts from lipocalin-2 deficiency mice: Restoration of mitochondrial function and phospholipids remodeling. *Am J Transl Res* 4:60–71.
31. Wang Y, et al. (2007) Lipocalin-2 is an inflammatory marker closely associated with obesity, insulin resistance, and hyperglycemia in humans. *Clin Chem* 53:34–41.
32. Wu G, et al. (2014) Elevated circulating lipocalin-2 levels independently predict incident cardiovascular events in men in a population-based cohort. *Arterioscler Thromb Vasc Biol* 34:2457–2464.
33. Walters AM, Porter GA, Jr, Brookes PS (2012) Mitochondria as a drug target in ischemic heart disease and cardiomyopathy. *Circ Res* 111:1222–1236.
34. Sareila O, Kelkka T, Pizzolla A, Hultqvist M, Holmdahl R (2011) NOX2 complex-derived ROS as immune regulators. *Antioxid Redox Signal* 15:2197–2208.
35. Lau AT, Wang Y, Chiu JF (2008) Reactive oxygen species: Current knowledge and applications in cancer research and therapeutic. *J Cell Biochem* 104:657–667.
36. Parkos CA (2016) Neutrophil-epithelial interactions: A double-edged sword. *Am J Pathol* 186:1404–1416.
37. Saha P, et al. (2017) Bacterial siderophores hijack neutrophil functions. *J Immunol* 198:4293–4303.
38. Gray MW, Burger G, Lang BF (2001) The origin and early evolution of mitochondria. *Genome Biol* 2:reviews1018.1–reviews1018.5.
39. Pearce RE, Cohen-Wolkowiez M, Sampson MR, Kearns GL (2013) The role of human cytochrome P450 enzymes in the formation of 2-hydroxymetronidazole: CYP2A6 is the high affinity (low K_m) catalyst. *Drug Metab Dispos* 41:1686–1694.
40. Liu JTC, et al. (2012) Lipocalin-2 deficiency prevents endothelial dysfunction associated with dietary obesity: Role of cytochrome P450 2C inhibition. *Br J Pharmacol* 165:520–531.
41. Richardson DR, et al. (2010) Mitochondrial iron trafficking and the integration of iron metabolism between the mitochondrion and cytosol. *Proc Natl Acad Sci USA* 107:10775–10782.
42. Miethke M, Marahiel MA (2007) Siderophore-based iron acquisition and pathogen control. *Microbiol Mol Biol Rev* 71:413–451.